Aquatic Mammals 2000, **26.3,** 212–228

Hearing capabilities of a beluga whale, *Delphinapterus leucas*

V. O. Klishin, V. V. Popov, and A. Ya. Supin

Institute of Ecology and Evolution, Russian Academy of Sciences, 33 Lenincky Prosp., 117071 Moscow, Russia

Abstract

Hearing sensitivity, frequency tuning, temporal resolution, and directional selectivity were measured in a beluga whale (*Delphinapterus leucas*) using evoked-potential methods. The animal had a U-shaped audiogram, similar other odontocetes, with high sensitivities (<75 dB re 1 μPa) from 32 kHz to 108 kHz; with the lowest threshold of 54.6 dB at 54 kHz. Frequency tuning curves were of equivalent rectangular quality (Q_{ER}) values from 27.2 at 32 kHz to 49.7 at 108 kHz center frequency (Q_{10dB} values from 14.0 to 25.5 respectively). Amplitude-modulation and rhythmic-click rates were reproduced by rhythmic evoked potentials with a cut-off frequency of 1400 Hz. Directional selectivity diagram was characterized by about 20-dB threshold increase at a 90° azimuth.

Key words: beluga, hearing.

Introduction

Although the auditory system of cetaceans attracts considerable interest, hearing capabilities of cetaceans have been studied in a limited number of species. Most available data concerns hearing sensitivity audiograms obtained psychophysically in a number of odontocetes: the bottlenose dolphin, *Tursiops truncatus* (Johnson, 1967), harbor porpoise, *Phocoena phocoena* (Andersen, 1970), killer whale, *Orcinus orca* (Hall & Johnson, 1971), Amazon river dolphin, *Inia geoffrensis* (Jacobs & Hall, 1972), beluga whale, *Delphinapterus leucas* (White *et al*., 1978; Awbrey *et al*., 1988; Johnson, 1992), false killer whale, *Pseudorca crassidens* (Thomas *et al*., 1988), Risso's dolphin, *Grampus griseus* (Nachtigall *et al*., 1995), Chinese river dolphin, *Lipotes vexillifer* (Wang *et al*., 1992), Pacific white-sided dolphin, *Lagenorhynchus obliquidens* (Tremel *et al*., 1998), and killer whale, *Orcinus orca* (Szymanski *et al*., 1999). These data were confirmed by evoked-potential studies in *Phocoena phocoena* (Popov *et al*., 1986), *Tursiops truncatus* (Popov & Supin, 1990*a*), *Delphinapterus leucas* (Popov & Supin, 1987), *Delphinus delphis* (Popov & Klishin, 1998), *Inia geoffrensis* (Popov & Supin, 1990*b*), and *Orcinus orca* (Szymanski *et al*., 1999).

Fewer data, however, are available on other characteristics of cetacean hearing such as frequency selectivity, temporal resolution, and directional selectivity. Most of these data have been obtained from *Tursiops truncatus*. In particular, frequency tuning was assessed in behavioral conditioning studies in *Tursiops truncatus* by measurement of the critical ratio and critical bands (Johnson 1968; Au & Moore 1990) and by tone-tone masking (Johnson, 1971) and in evoked-potential studies using the tuning-curve (Supin *et al*., 1993; Popov *et al*., 1995) and notch-noise paradigms (Popov *et al*., 1997). Temporal resolution was studied in *Tursiops truncatus* as well using the evoked-potential technique (Dolphin *et al*., 1995*a,b*; Supin & Popov, 1995; Popov & Supin, 1997, 1998). Because frequency tuning, temporal resolution, and directional selectivity rarely have been investigated in other cetaceans, we undertook this study in the beluga whale, *Delphinapterus leucas.*

A previous attempt was made to study frequency tuning in a beluga whale using the critical-ratio method (Johnson *et al*., 1989). However, the critical ratio is a poor estimate of frequency tuning because small changes in the signal-in-noise detection efficiency influence the critical ratio as much as large changes in frequency tuning. Temporal resolution was studied in the beluga whale using the modulation transfer function paradigm (Dolphin *et al*., 1995*a,b*), but only using low-frequency carriers.

In the study presented herein, we concentrated on investigating frequency tuning, temporal resolution, and directional selectivity in the beluga whale using the evoked-potential method. Although hearing thresholds in beluga whales were studied earlier, we repeated those measurements in the present study as well.

Materials and Methods

Subject

The subject was an adult beluga whale (*Delphinapterus leucas*), male of 370 cm body length and

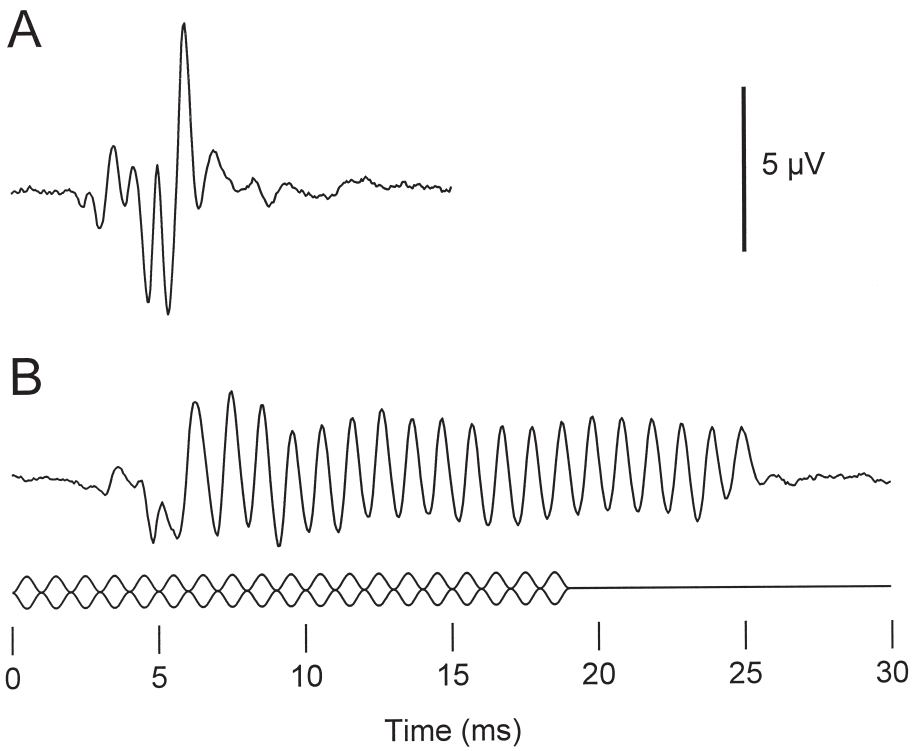

Figure 1. Evoked responses to a single click (A) and sinusoidally amplitude-modulated tone (B). Stimulus levels are 140 dB re 1 μPa. In (A), the stimulus instant corresponds to the beginning of the record. In (B), stimulus envelope is shown under the evoked-response record (19 cycles of 1000-Hz modulation rate, the carrier frequency 64 kHz).

about 500 kg body mass. The animal was adapted to captivity; before the study it was kept for two years in a dolphinarium. The study was carried out in the Utrish Marine Station of the Russian Academy of Sciences (Black Sea coast). The animal was kept in a sea-water pool 9 × 4 × 1.2 m.

Experimental conditions

During experimentation, the water level in the pool was lowered to 40 cm depth. The animal was supported by a stretcher so that the dorsal part of the body and blowhole were above the water surface. The stretcher was made of sound-transparent material (thin net). The experiments lasted for 2 to 3 hr, after which the water level was returned to the normal value (1.2 m) and the animal released.

Stimuli

Stimuli were clicks, short tone pips, or sinusoidally amplitude-modulated tones. Clicks were generated by activation of a piezoceramic transducer (B&K 8104 hydrophone) with rectangular pulses of 10 μs. Pips were generated digitally at a 500-kHz sampling rate and played through a D/A converter, amplifier, attenuator, and the same transducer. Their carrier frequency varied from 8 kHz to 128 kHz, and their envelope was one 0.5-ms cycle of a cosine function. Amplitude-modulated tone bursts were generated and played in the same manner. They were presented in bursts of 18 ms plus time to the end of the last modulation cycle. Modulation rate varied from 125 to 2000 Hz, in 62.5-Hz steps. Modulation depth was 100%. Stimuli were repeated at a rate of $10\ s^{-1}$.

In masking experiments, masking signals were continuous tones of various frequency and level. Probe and masker were not coherent. The probe and masker were independently attenuated, mixed and emitted through one and the same transducer.

The stimulating transducer was placed 1 m from the animal's head, at a depth of 20 cm. Thus, sound spread in 40-cm deep water was close to that in a flat layer. In all experiments except in measurements of directional selectivity, the transducer was placed at the longitudinal head axis; in the latter

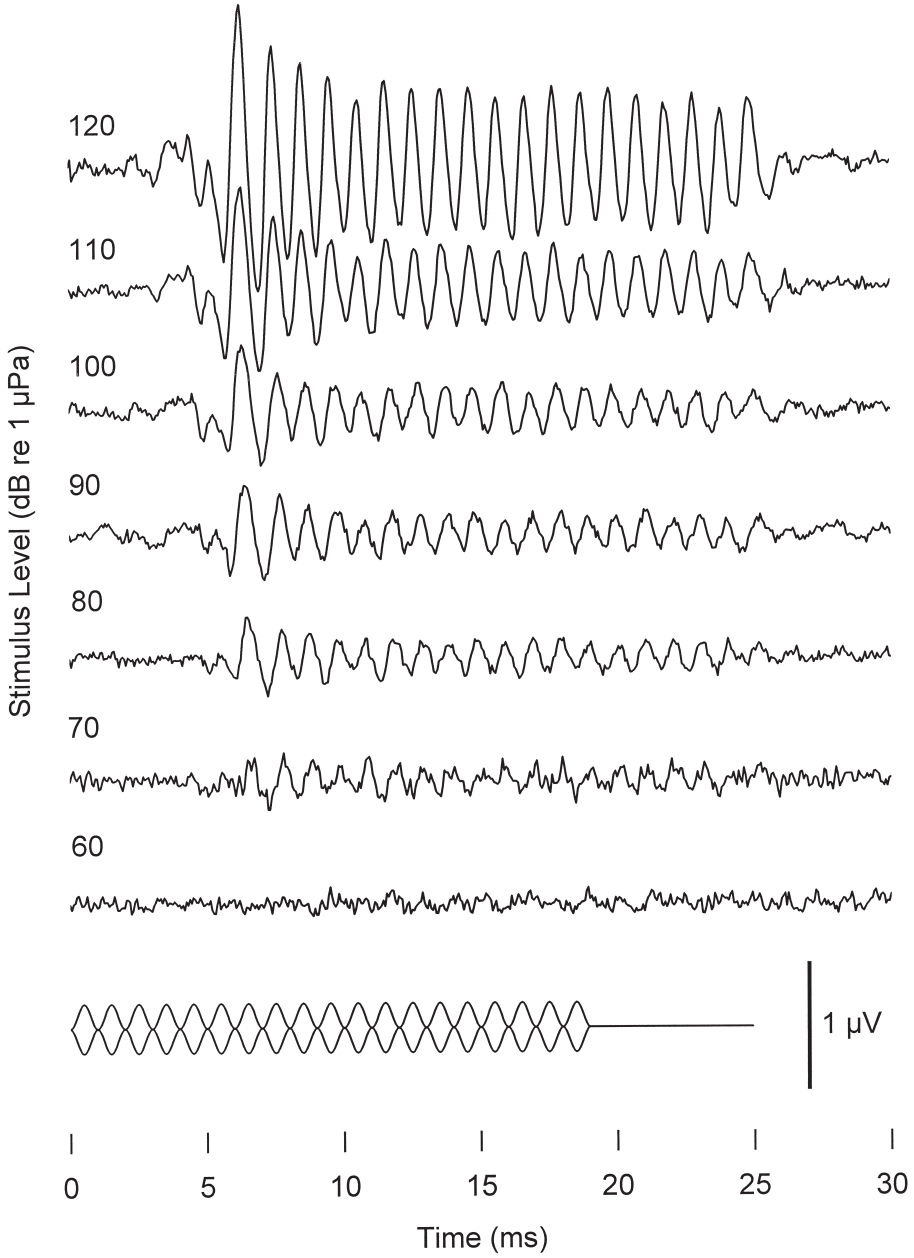

Figure 2. Examples of EFR to a sinusoidally amplitude-modulated carrier of 64 kHz. Stimulus levels are indicated near the records, in dB re 1 µPa. The lowest record is the stimulus envelope.

experiments, it took position on a horizontal arc of 1 m radius, centered on the melon center.

Stimuli were monitored through a hydrophone located near the animal's head with a passband of 150 kHz. Stimulus intensity was specified in dB re 1 µPa of RMS sound pressure.

Evoked potential collection

Evoked potentials were recorded using 1-cm disk electrodes secured at the body surface with a drop of adhesive electric-conductive gel. The active electrode was placed at the head vertex, just behind the blowhole. Pilot studies showed that this

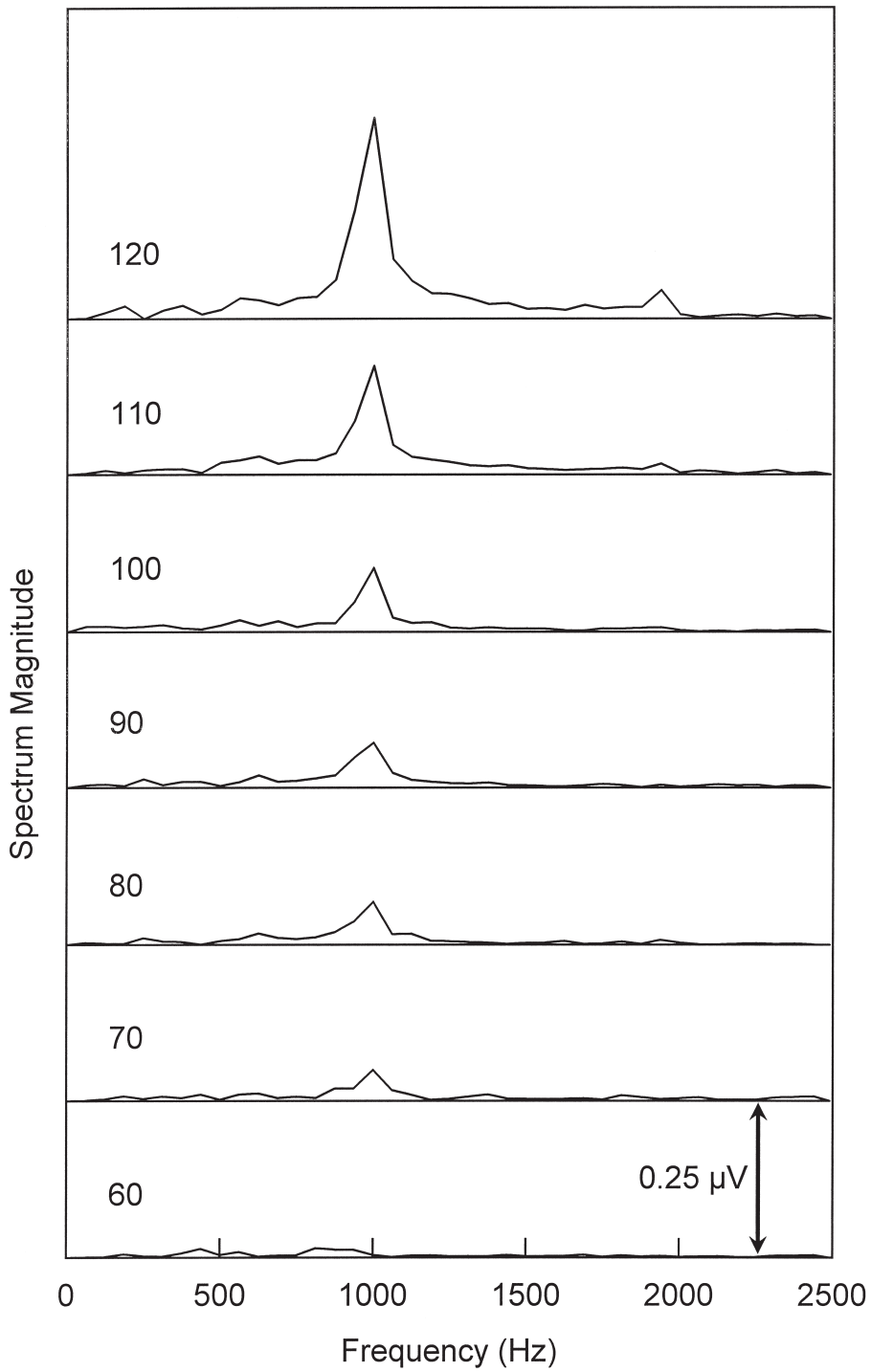

Figure 3. Fourier spectra of records shown in Fig. 2. Stimulus levels are indicated near the spectra, in dB re 1 μPa.

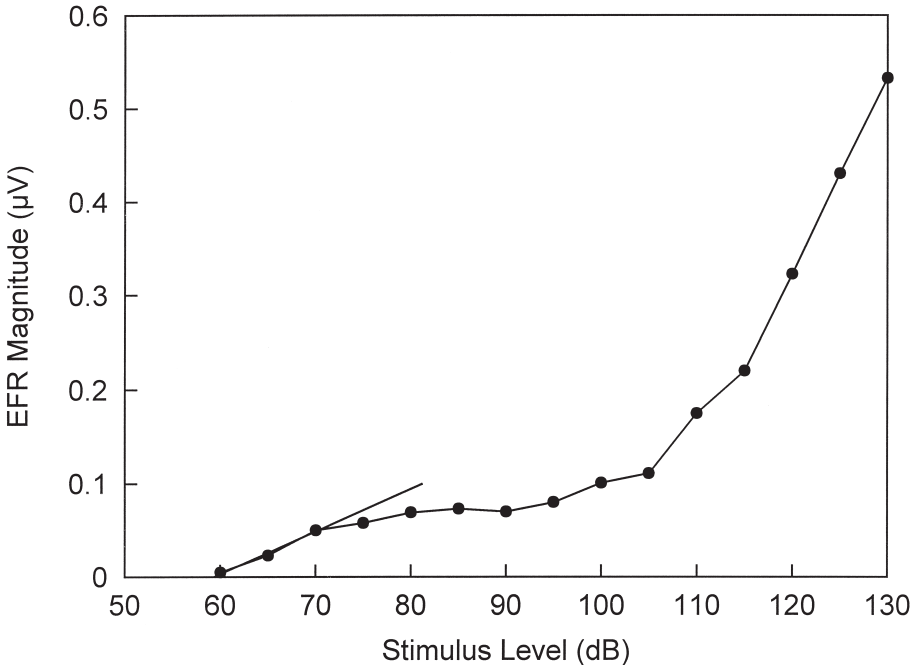

Figure 4. EFR amplitude as a function of amplitude-modulated tone level. Stimulus carrier 64 kHz, modulation rate 1000 Hz. A straight line—the regression line approximating the plot within a region of 60 to 70 dB.

electrode position is the most effective for ABR recordings. The reference electrode was placed at the back (both electrodes above the water surface). The recorded potentials were amplified by 70 dB within a passband of 5000 Hz (flat frequency response to 3000 Hz, − 3 dB at 5000 Hz with 6 dB/oct slope above this point), digitized using an A/D converter and averaged using a personal computer. The record window was 10 ms when responses to single clicks or pips were recorded and 30 ms when responses to amplitude-modulated bursts or click trains were recorded. One thousand sweeps were averaged to collect one evoked-response record.

Results

Single and rhythmic ABR waveform

Sound clicks and short pips evoked ABR (Fig. 1 A) very similar to that described in other dolphin species at similar electrode positions (Popov & Supin, 1990*a*; Popov & Klishin, 1998). It consisted of a few waves lasting less than 1 ms. At high stimulus intensities (60–80 dB above threshold), the response onset latency (including the acoustic delay of 0.7 ms) was 2.1 ms; i.e., its physiological latency was as short as 1.4 ms. Response peak-to-peak amplitude reached 10 μV when the stimulus was a wide-band high-intensity click. Narrow-band stimuli (cosine-enveloped pips) evoked responses of lower amplitude; up to 3–5 μV, depending on the carrier frequency.

Sinusoidally amplitude-modulated tone bursts evoked pronounced rhythmic responses which followed the modulation rate—the envelope-following response, EFR (Fig. 1 B). The tone burst onset evoked a small transient on-response which after a few milliseconds was replaced by the quasi-sustained EFR. Both the start and end of the response appeared with a few ms lag relative to the stimulus. The response-free initial part of the records indicates that the records were not contaminated by artifacts. As was shown previously in the bottlenose dolphin (Supin & Popov, 1995), this rhythmic response is composed of a sequence of ABRs to each modulation cycle. In particular, it is well visible in Fig. 1 B that the response lag is equal to the latency of the main (the latest) ABR waves.

Hearing thresholds

To measure hearing thresholds, we used not single ABRs, but rhythmic responses to amplitude-modulation tones (EFR), because this stimulation mode and response type has several advantages: (i) the level of a long tone burst can be specified unambiguously by RMS sound pressure, whereas effectiveness of a short pulse depends on both its

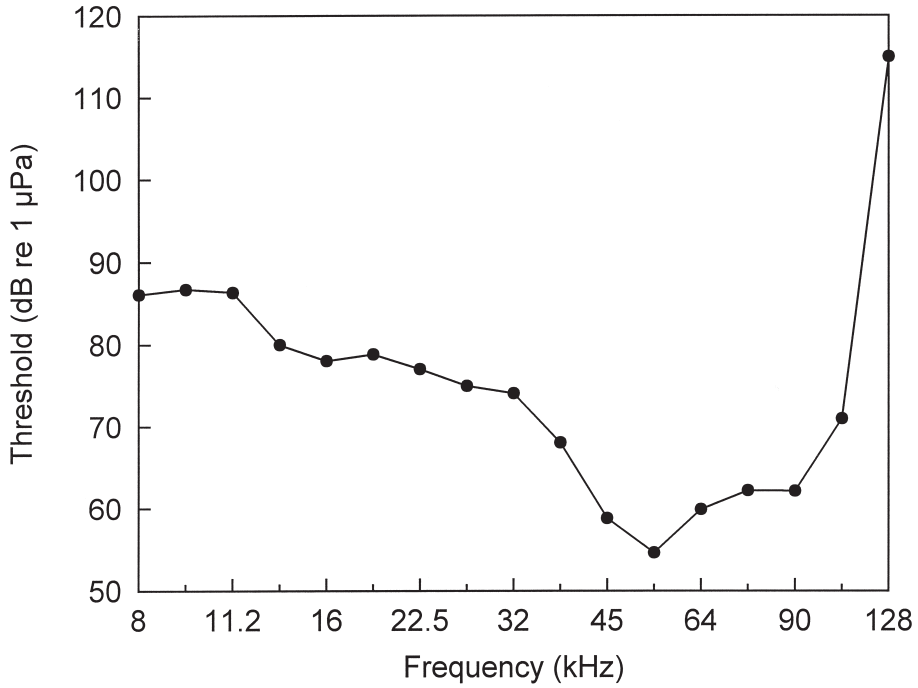

Figure 5. Audiogram of the beluga whale. Thresholds in dB re 1 µPa.

sound pressure and duration; (ii) very low response amplitude to near-threshold stimuli can be measured precisely, using Fourier transform and evaluation of the magnitude of a spectral peak at the modulation frequency.

To measure hearing threshold at a certain frequency, EFR was recorded to amplitude-modulated tone bursts of that carrier frequency and of various sound levels. Modulation rate was always kept of 1000 Hz since this rate was effective to evoke EFR. Sound level decreased in 5-dB steps until the response disappeared in noise. This procedure is illustrated in Figure 2 which presents EFR records at various sound levels (only records separated by 10-dB steps are shown). In each record, a 16-ms fragment (from 7.5 to 23.5 ms after the stimulus onset) was Fourier transformed to obtain a frequency spectrum (Fig. 3). This position of the window for Fourier transform was selected since it contained a major part of the rhythmic response, but did not include the initial transient part of the response. The magnitude of the peak at 1000 Hz (the modulation frequency) was taken to express the response magnitude in terms of RMS voltage. As a result, response magnitudes were obtained as a function of stimulus level for a given carrier frequency (Fig. 4).

A typical EFR-magnitude dependence on stimulus level had three branches. At middle levels (70 to 105 dB in Fig. 4), EFR magnitude was slightly dependent on stimulus level; as was shown previously in the bottlenose dolphin (Supin & Popov, 1995), within this level range, EFR more depends on modulation depth rather than on stimulus level. At high levels (110 dB and higher in Fig. 4), EFR magnitude rose steeply. At low levels (below 70 dB in Fig. 4), EFR magnitude fell steeply with the level decrease.

Using the magnitude-vs-level function, hearing thresholds were estimated at each of the tested frequencies. Two threshold estimates were used. The first one was a stimulus level at which the response magnitude reached a certain arbitrary criterion. Spectra of the type presented in Figure 3 allowed threshold criterion as low as 0.01 µV. Thresholds were found by interpolation between the stimulus levels giving response magnitude just above and just below the criterion value. In the case exemplified in Figure 4, this threshold estimate was 61.4 dB.

Another way to estimate a threshold follows. The low-level branch of a plot like that in Figure 4 was approximated by a regression line which was extrapolated to the zero response magnitude. This point was taken as a threshold estimate. As an example, the regression line drawn in Figure 4 through points at 60, 65, and 70 dB indicates a threshold of 59.3 dB. Estimates obtained in these two ways differed by 1.5–2 dB. Below we present

data obtained in the second way (regression line) since this mode of threshold estimation is free of arbitrary selection of the threshold criterion.

Thresholds were measured at frequencies from 8 kHz to 128 kHz, in quarter-octave steps. The resulting audiogram is presented in Figure 5. The lowest threshold estimate (54.6 dB) was obtained at 54 kHz. Within a range of 32 kHz to 108 kHz, thresholds remained below 75 dB; then thresholds rose slowly with decreasing the frequency (around 86 dB at 8 kHz–11 kHz) and very steeply with increasing frequency (>110 dB at 128 kHz).

Frequency tuning

Frequency tuning was measured using the simultaneous tone-tone masking paradigm. As well as in the preceding series, sinusoidally amplitude-modulated tone bursts were used as probes. Modulation rate was 1000 Hz, and the probe level was kept at 40 dB above the hearing threshold at the given carrier frequency. At a given probe frequency, masker frequency and level were varied to find masking thresholds as a function of masker frequency. Figure 6 depicts an EFR evoked by a probe without a masker (A) and in the presence of various maskers (B, C). Without a masker, the probe stimulus evoked a response of about 0.5 υV peak-to-peak amplitude (0.12–0.15 μV RMS magnitude) (A). The same stimulus in a masker background evoked a smaller response. As the masker level increased, the response diminished until it disappeared in noise.

The masking was the most effective when the probe and masker frequencies were equal (64 kHz in Fig. 6B). In this case, the complete masking required a masker level of about 10 dB above the probe level (50 dB re hearing threshold). When the masker and probe frequencies were different, the masking was less effective. In Figure 6C, the masker frequency was 67 kHz while that of the probe was 64 kHz, and the masking required masker levels of 25 dB higher than in the preceding case.

Using such records, masking thresholds were estimated in the same manner as hearing thresholds in the preceding series; i.e., EFR records were Fourier transformed, peak magnitude at 1000 Hz was measured, and the masker level was found which suppressed the probe response to a 0.01 μV criterion level. This procedure was repeated at various masker frequencies to yield a complete tuning curve. To draw the curve, the experimental points were approximated by the rounded-exponential (*roex*) function which is widely used to approximate auditory filters:

$$W(g)=(1+pg)e^{-pg} \quad (1)$$

where, $W(g)$ is the filter form, g is the normalized frequency deviation from the center, and the term p determines the filter tuning (Patterson et al., 1982). The line drawn according to Eq. (1) was fitted to experimental data, for which purpose the frequency and level of the curve peak and the parameter p were adjusted to minimize the mean-square deviation from the data.

A family of tuning curves obtained in such a way is shown in Figure 7. The curves were obtained at probe frequencies varied by quarter-octave steps within a range of 32 kHz to 108 kHz. All the curves peaked at or near the probe frequency. The parameter p varied from 88.2 (at 45 kHz probe frequency) to 198.7 (at 108 kHz).

An adopted metric of filter width is the equivalent rectangular bandwidth (ERB). For the *roex* filter, ERB is:

$$W_{ER}=4f/p \quad (2)$$

where, W_{ER} is ERB and f is the center frequency of the filter. Thus, filter tuning is defined as the center frequency divided by ERB:

$$Q_{ER}=f/W_{ER}=p/4 \quad (3)$$

Another convenient measure of tuning is a $Q_{10\mathrm{dB}}$ value, that is, the center frequency divided by the bandwidth at a level of (− 10 dB. For the *roex* function, $Q_{10} \approx p/7.78$. Thus, the found values of the parameter p correspond to Q_{ER} of 22.1 to 49.7 and $Q_{10\mathrm{dB}}$ of 11.3 to 25.5 (Fig. 8). The tuning dependence on probe frequency exhibited an obvious trend (except a small dip at 45 kHz); from $Q_{\mathrm{ER}}=22.7$ ($Q_{10\mathrm{dB}}=14.0$) at 32 kHz to $Q_{\mathrm{ER}}=49.7$ ($Q_{10\mathrm{dB}}=25.5$) at 108 kHz.

Temporal resolution

To assess temporal resolution of the auditory system, its ability to transfer rhythmic sound modulation or sound pulse rates, i.e., the modulation rate transfer function (MTF) was studied. Two kinds of rhythmic stimuli were used; sinusoidally amplitude-modulated tones and wide-band clicks trains.

EFR to amplitude-modulated tones was recorded at modulation rates from 125 to 2000 Hz varied by steps of 62.5 Hz. Figure 9 presents representative

Figure 6. EFR suppression by maskers. A: unmasked EFR evoked by a probe stimulus of 64 kHz frequency, 40 dB above threshold. B: responses to the same probe in the background of 64-kHz masker. C: The same in 67-kHz masker. The lowest record is the stimulus envelope. Masker levels (dB re probe threshold) are shown near the curves.

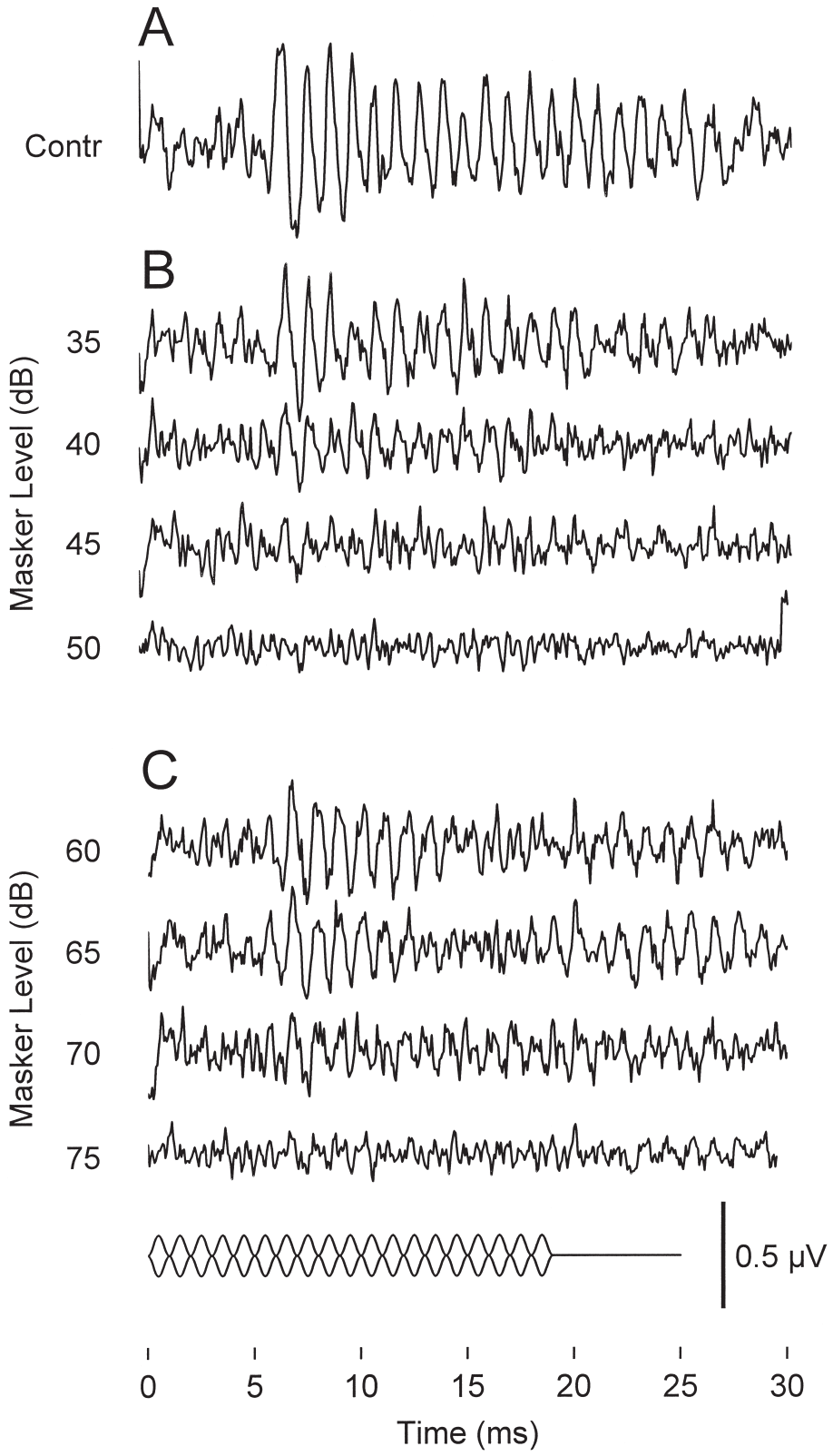
A
Contr
B
Masker Level (dB)
35
40
45
50
C
Masker Level (dB)
60
65
70
75
0.5 µV
0
5
10
15
20
25
30
Time (ms)

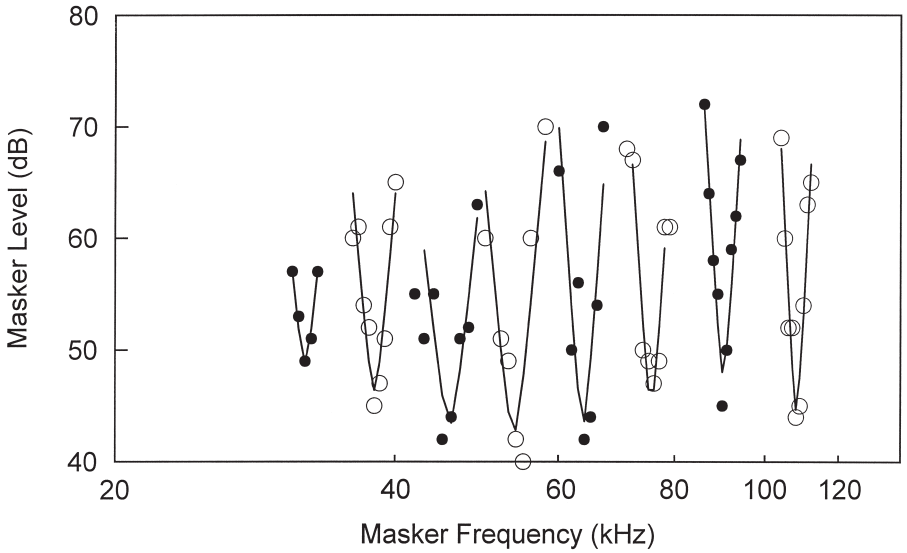

Figure 7. Tuning curves of hearing in the beluga whale: criterion masker levels (in dB re probe response threshold) as functions of the masker frequency. The curves were obtained (from left to right) at probe frequencies of 32, 38, 45, 54, 64, 76, 90, and 108 kHz; probe level was always of 40 dB above the response threshold. Dots represent experimental data (to distinguish points belonging to neighboring curves, they are shown by filled and open circles alternatively); the curves show the least-mean-square approximations by *roex* functions.

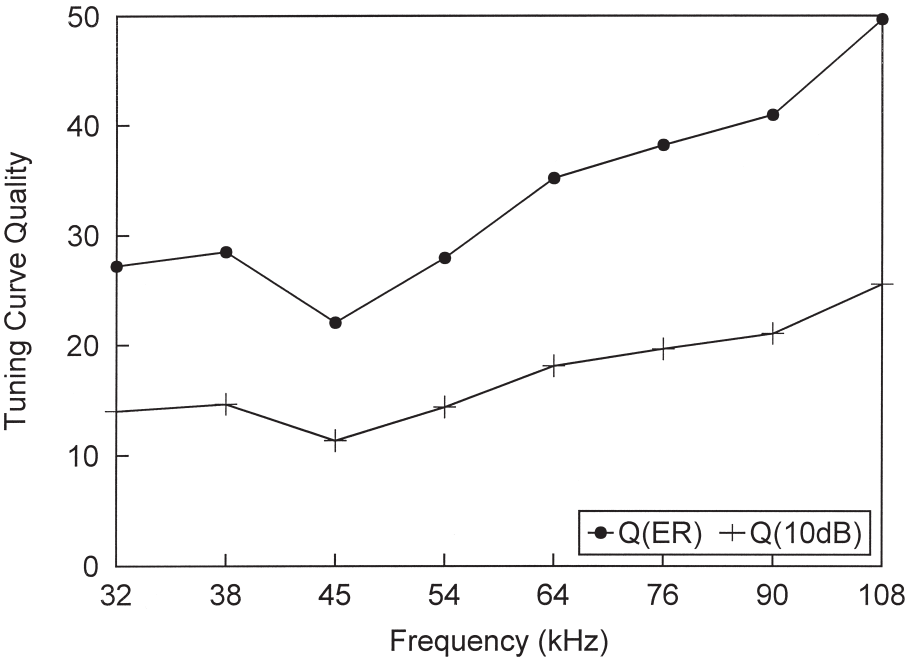

Figure 8. Tuning curve quality as a function of frequency. Two estimates are presented: equivalent rectangular quality (Q_{ER}) and 10-dB quality (Q_{10dB}).

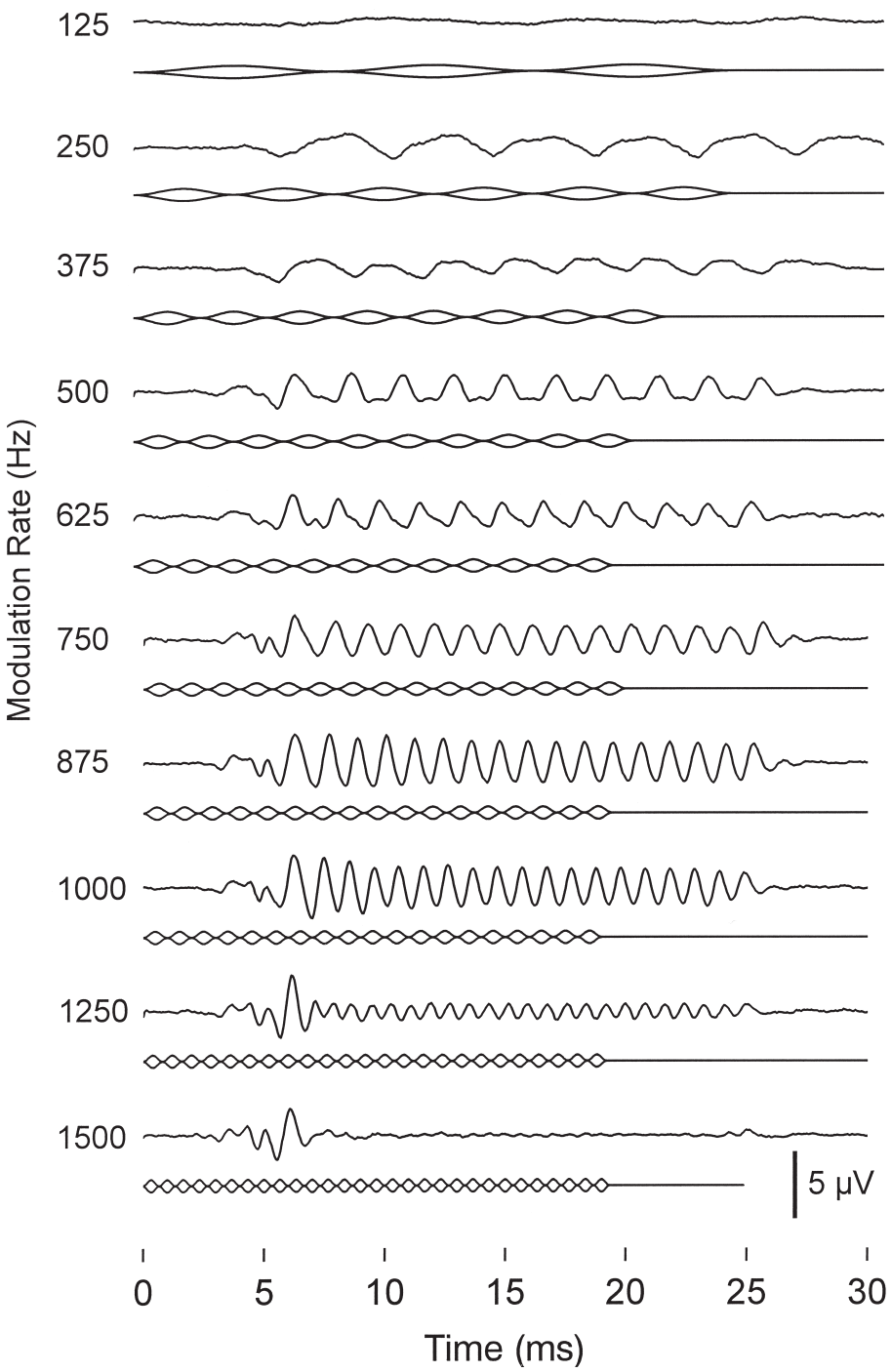

Figure 9. EFR examples at various modulation rates. Stimuli—sinusoidally amplitude-modulated tone bursts of 64 kHz, 140 dB level (80 dB above the response threshold). Modulation rates (Hz) are shown near the records. In each record pair, the upper one is the EP record and the lower one is the stimulus envelope.

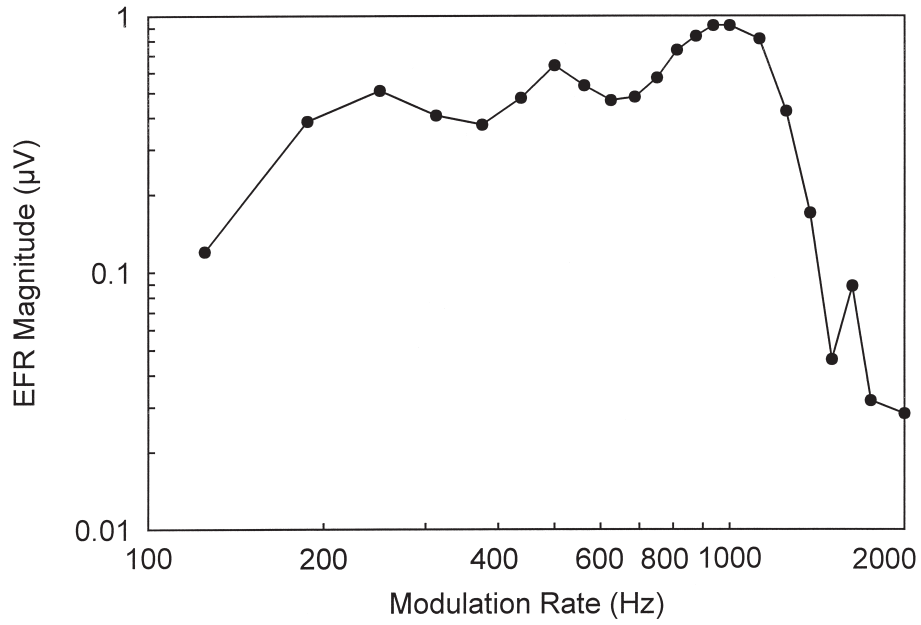

Figure 10. Modulation transfer function: EFR magnitude dependence on modulation rate. Stimulus parameters as in Fig. 9.

EFRs at several modulation rates. It shows robust rhythmic responses at rates up to 1250 Hz; even at a rate of 1500 Hz, small but noticeable response appeared.

To evaluate EFR magnitude to a given stimulus, a 16-ms part of the record, from 7.5 to 23.5 ms after the burst onset, was Fourier transformed to find the magnitude of the component (fundamental) at the modulation rate. Note that the analyzed window always contained a whole number of response cycles; from two cycles at a rate of 125 Hz to 32 cycles at 2000 Hz. Figure 10 shows the EFR magnitude defined in such a way, as a function of modulation rate. The plot was a multipeak function with small peaks at modulation rates of 250, 500 and 1000 Hz and troughs between. The function declined sharply at rates above 1125 Hz, and was hardly detectable at 2000 Hz. A 10-fold decrease of the response magnitude (relative to the highest peak at 1000 Hz) was at a modulation rate higher than 1375 Hz (around 1400 Hz).

Responses to rhythmic clicks were recorded under similar conditions; clicks were presented in bursts of 18 ms plus time to the end of the last cycle; their rate varied from 125 to 2000/s by steps of 62.5/s. Figure 11 presents representative response examples at several click rates. It shows pronounced responses at rates from 125 to 1000/s; at a rate of 1250/s responses are still of significant amplitude. At low stimulation rates (125–250/s), the responses look like a sequence of separate ABRs; at higher rates, individual ABRs fuse into a continuous rhythmic response like EFR.

The magnitude of the Fourier fundamental is not an appropriate measure for low-rate click-evoked response sequences: this measure decreases with rate decrease, whereas ABR amplitude remains high. Therefore, we used peak-to-peak amplitude as a measure of this response type. The amplitude was calculated as a mean peak-to-peak amplitude of all response cycles within a temporal window from 7.5 to 23.5 ms after the burst onset. Figure 12 shows the ABR amplitude defined in such a way, as a function of pulse rate. Note that peak-to-peak measure gives higher voltage values than RMS measure (for a sinusoid, the ratio is $2\sqrt{2} \approx 2.8$). Even with correction for this factor, ABR evoked by short clicks are higher in amplitude than EFR evoked by modulated tone (compare Figures 10 and 12). The plot had a plateau at low rates, then small peaks at rates of 400–500 and 800–1000/s, and sharp decay at rates above 1125/s. A 10-fold decrease of the response magnitude (relative to the low-rate plateau) was at a pulse rate higher than 1375/s (around 1400/s). Thus, both amplitude-modulated tones and wide-band clicks revealed one and the same cut-off frequency, around 1400 Hz.

Directional selectivity

To investigate directional selectivity of hearing, thresholds were measured at various azimuthal

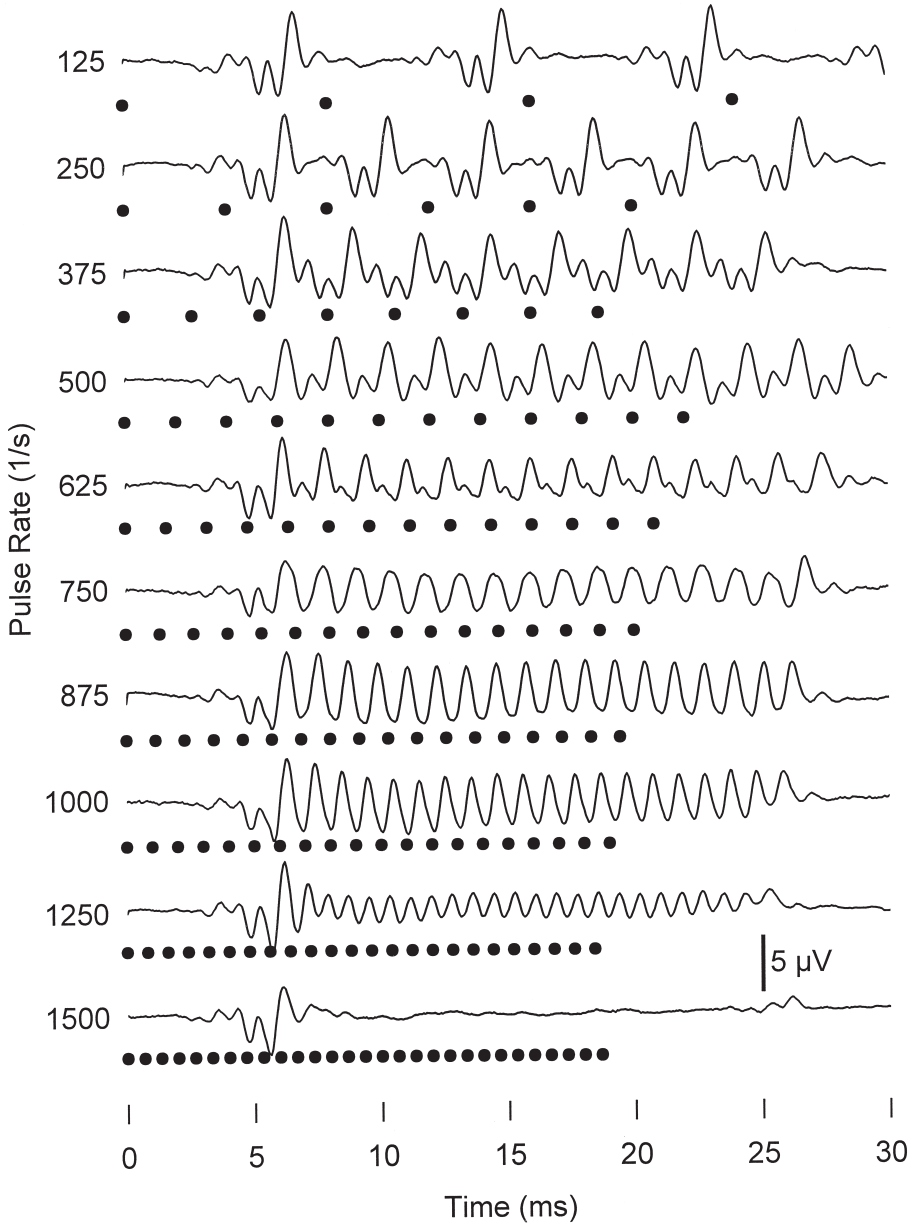

Figure 11. ABR examples at various pulse rates. Stimuli—short wide-band pulses 80 dB above the response threshold. Pulse rates (1/s) are shown near the records. Under the records, points show instants of pulse presentation.

positions of the transducer around the animal's head. Contrary to preceding series, long amplitude-modulated tone bursts were not used in this series because a distortion of results by echo from the pool walls is particularly unacceptable for these measurements. Therefore, we used short (0.5-ms) tone pips to evoke ABR. Due to short ABR duration, a response to directly impinging sound could be separated easily from that to echo which was delayed by at least a few ms.

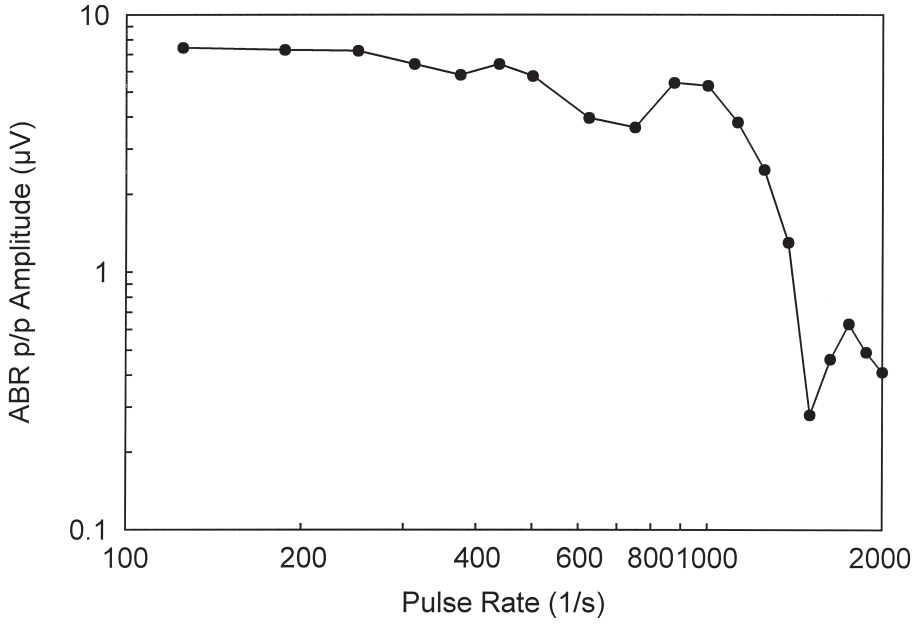

Figure 12. ABR amplitude dependence on pulse rate. Stimulus parameters are as in Fig. 11.

For threshold measurement, stimulus level decreased in 5-dB steps from a level well above the anticipated ABR threshold to a sub-threshold level. This resulted in progressive decrease of ABR amplitudes until its disappearance in noise. Near threshold, ABR amplitude was comparable with the background EEG noise. To extract a low-amplitude ABR waveform and measure the amplitude with a satisfactory precision, the following procedure was used (Fig. 13). A cross-correlation function was calculated between a standard high-amplitude ABR waveform (Fig. 13A) and the measured record (Fig. 13B). Since ABR of lower amplitude had longer latency, this function peaked at a delay from 0 to 0.25 ms (Fig. 13C). This peak value was taken as a measure of ABR waveform weight in the analyzed record. Using this technique, ABR amplitudes as low as 0.05–0.07 μV could be extracted from noise. We used an arbitrary selected level of 0.15 μV as a threshold criterion.

Using this technique, ABR thresholds were measured at sound-source azimuthal positions within a range of ± 105° from the midline. Positions were varied in steps of 15°. Measurements were made at pip carrier frequencies of 16, 22.5, 32, 45, 64 and 90 kHz, and also for short wideband clicks. Since no systematic difference was found between thresholds at symmetrical left and right sound-source positions, these data were averaged.

The results obtained in this series are summarized in Figure 14 which presents thresholds as a function of sound-source azimuth. At all probe frequencies, the lowest thresholds were observed at zero azimuth (midline). With azimuth increase, threshold increased. At the largest tested azimuth of 105°, threshold elevation to tone pips varied from 22 to 31 dB at different frequencies; at a 90°-azimuth the elevation was around 20 dB. We failed to notice a systematic dependence of directional diagrams on frequency (Fig. 14A); although absolute threshold values depended on frequency in a manner described above (which manifested itself in plot shift along the ordinate axis), the slopes of the plots did not differed markedly. Responses to wideband clicks exhibited the same dependence on azimuth with threshold elevation as high as 27 dB at 105° azimuth and around 20 dB at a 90° azimuth (Fig. 14B).

Discussion

Audiogram

The audiogram of the beluga whale obtained in the present study by the evoked-potential method to AM tones is in a good agreement although does not coincide exactly with that obtained by White *et al.* (1978) and Johnson (1992) in psychophysical measurements. The lowest threshold obtained herein (below 54.6 dB re 1 μPa at 54 kHz) is a

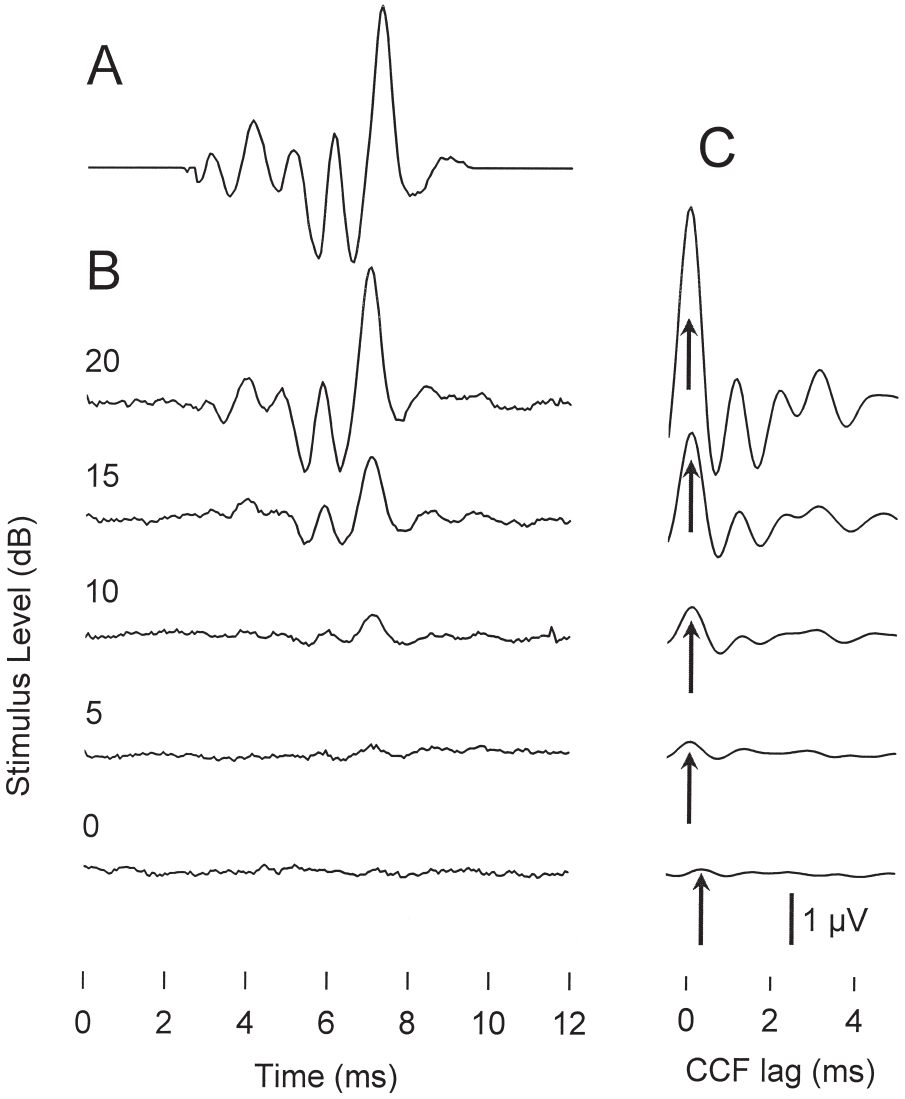

Figure 13. Procedure of ABR amplitude measurement using cross-correlation functions. A: standard ABR waveform (a response to high-level click). B: measured records at stimulus levels from 20 to 0 dB re arbitrary response threshold. C: cross-correlation functions (CCF) between the records in (B) and standard waveform (A). Arrows indicate the measured CCF peak. Note well detectable CCF peaks at low stimulus levels (0–5 dB) whereas ABR waveforms at these stimulus levels are comparable with noise.

few dB higher than that found psychophysically, but limited data does not allow us to conclude whether this difference is due to scatter in individual hearing sensitivity, or experimental conditions, or method sensitivity. Audiograms obtained previously by the evoked-potential method (Popov & Supin, 1987) were very similar in form with that presented herein, but thresholds were higher (above 60 dB re 1 μPa). However, it should be taken into account that those thresholds were measured using short pips which are difficult to assess in terms of effective sound pressure.

In general, combining all available data makes it possible to state that the beluga whale is similar to a number of other odontocetes having a wide frequency range of hearing (above 100 kHz), although this range is a little less than those of small cetaceans.

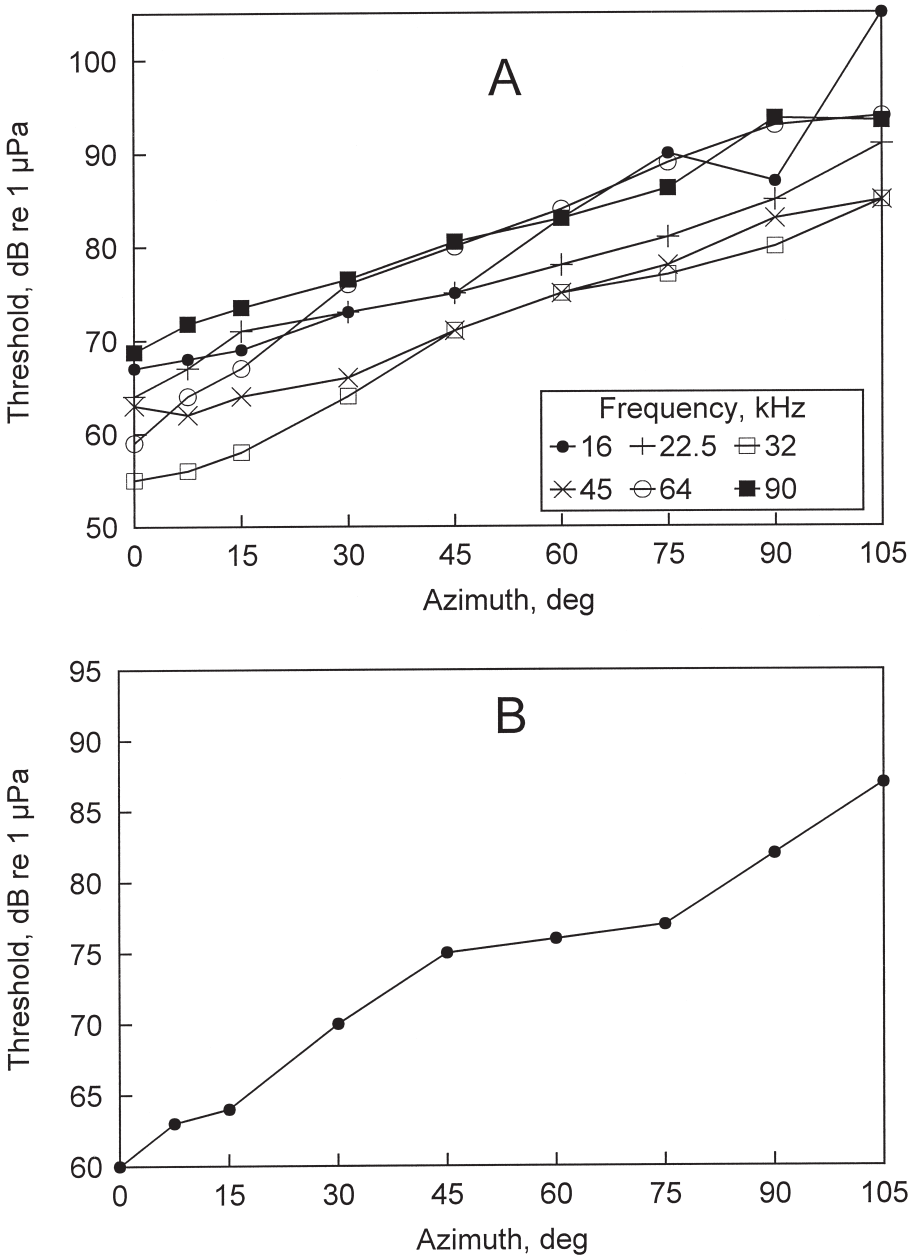

Figure 14. ABR thresholds (in dB re 1 µPa) as a function of sound source azimuthal position. A: data for tone pips with carriers from 16 to 90 kHz, as indicated in the legend. B: data for short clicks.

Tuning curves

According to data presented herein, frequency tuning of the beluga whale is extremely acute. Very acute tuning estimates have already been obtained in bottlenose dolphins (Supin *et al.*, 1993; Popov *et al.*, 1995, 1997): Q_{10dB} were higher than 15 and Q_{ER} were about 35 (for comparison, in humans Q_{ER} is about 10). In the beluga whale, tuning curves were even more acute than in bottlenose dolphins (Q_{ER} up to 50 at high frequencies). It is possible that this acute frequency tuning explains better detection of echolocation signals in noise (Turl *et al.*, 1987) and reverberation (Turl *et al.*, 1991) by belugas than by bottlenose dolphins.

It should be noted that these estimates were obtained using the tone-tone masking paradigm. In some conditions, this paradigm can overestimate frequency tuning due to the so-called off-frequency listening effect. However, it was shown in bottlenose dolphins that in conjunction with the evoked-response technique, the tone-tone masking gives frequency-tuning estimates very similar to those obtained with the notch-noise masking which is free of the off-frequency listening (Popov *et al*., 1997). This indicates that in evoked-response experiments, the off-frequency listening does not influences results even in conditions of tone-tone masking. So we can suppose that the frequency-tuning estimates obtained herein under similar conditions reflect true frequency selectivity of the beluga whale.

Temporal resolution

Temporal resolution in the beluga whale, as revealed by both amplitude-modulation and rhythmic-click tests, was rather high; cut-off frequency was around 1400 Hz. It is a little lower than in the bottlenose dolphin (Supin & Popov, 1995; Popov & Supin, 1998) and common dolphin (Popov & Klishin, 1998) which featured a cut-off frequency of about 1700 Hz, however higher than in the killer whale which has a cut-off frequency of about 1000 Hz (Szymanski et al., 1998). Thus, high temporal resolution seems to be a common feature of many, if not all, odontocetes and yet with some differences between them.

It is remarkable that lower temporal resolution in the beluga (as compared with the bottlenose dolphin) is associated with higher frequency resolution. It may reflect a reciprocal relationship between the frequency tuning and temporal resolution, i.e., the narrower passband of the auditory filters (better frequency tuning), the lower the limit of transferred modulation rate (worse temporal resolution). Indeed, within a rather wide frequency range (from 45 kHz to 108 kHz), frequency tuning of the beluga corresponds to the equivalent rectangular bandwidth of about 2 kHz (at 45 kHz, Q_{ER} was 22; at 108 kHz, it was around 50); i.e., $\pm$ 1 kHz from the center frequency. Such filters transfer modulation rates higher than 1 kHz with marked attenuation. The precise relation between the filter attenuation and evoked-response amplitude is not known, nevertheless, a 10-fold response amplitude decrease at 1400-Hz modulation rate can be taken as a satisfactory agreement with the theoretical prediction. In the bottlenose dolphin, Q_{ER} of around 35 at 90 kHz (Popov *et al*., 1997) corresponds to the filter bandwidth of $\pm$ 1.4 kHz, which is in almost the same relation to the cut-off modulation rate (1700 Hz) as in the beluga. It means that the relation between the frequency and temporal resolutions in the odontocete auditory system is close to the theoretical limit.

Directional selectivity

Directional selectivity function in the beluga was of the same order as those in a several other odontocetes: *Tursiops truncatus, Sotalia fluviatilis, Inia geoffrensis* (Popov & Supin, 1990*c*): at an azimuth of 90°, threshold increased to about 20 dB above that at the zero azimuth. Although some differences in directivity diagrams do exists among these species, there is no evidence that this difference markedly exceeds a natural variability. So it seems that such degree of acuteness of directional selectivity is a common feature of many odontocetes.

An unexpected result is that directional selectivity did not changed systematically with frequency. Interpretation of hearing directivity in terms of a receiving aperture (Au, 1993) predicts directivity increase with frequency, which was really observed in other dolphin species. We can not explain the result obtained herein by imperfect experimental pool since it provided a normal dependence of threshold on azimuthal sound-source position. We can not either explain it by imperfect stimulus characteristics (spectrum splatter) since they provided a normal dependence of thresholds on frequency. So this point needs further investigation.

Acknowledgments

The study was supported by the Russian Foundation for Basic Research, Grant number 97-04-49024 and 00-04-48879. Authors thank the Utrish Dolphinarium (Moscow, Russia) for possibility to investigate the animal.

Literature Cited

Andersen, S. (1970) Auditory sensitivity of the harbour porpoise, *Phocoena phocoena*. *Invest. Cetacea* **2**, 255–258.

Au, W. W. L. (1993) *The Sonar of Dolphins*. Springer, New York, 277 pp.

Au, W. W. L. & Moore, P. W. B. (1990) Critical ratio and critical band width for the Atlantic bottlenose dolphin. *J. Acoust. Soc. Am*. **88**, 1635–1638.

Awbrey, F. T., Thomas, J. F. & Kastelein, R. A. (1988) Low-frequency underwater hearing sensitivity in belugas, *Delphinapterus leucas*. *J. Acoust. Soc. Am*. **84**, 2273–2275.

Dolphin, W. F., Au, W. W. L. & Nachtigall, P. (1995*a*) Modulation transfer function to low-frequency carriers in three species of cetaceans. *J. Comp. Physiol. A* **177**, 235–245.

Dolphin, W. F., Au, W. W. L., Nachtigall, P. E. & Pawloski, J. (1995*b*) Modulation rate transfer functions to low-frequency carriers in three species of cetaceans. *J. Comp. Physiol. A*, **177**, 235–245.

Hall, J. D. & Johnson, C. S. (1971) Auditory thresholds of a killer whale, *Orcinus orca* Linnaeus. *J. Acoust. Soc. Am*. **51**, 515–517.

Jacobs, D. W. & Hall, J. D. (1972) Auditory thresholds of a fresh water dolphin, *Inia geoffrensis* Blainvsille. *J. Acoust. Soc. Am*. **51**, 530–533.

Johnson, C. S. (1967) Sound detection thresholds in marine mammals. In: W. N. Tavolga (ed.) *Marine Bio-Acoustics*. Vol. 2, pp. 247–260. Pergamon Press, New York.

Johnson, C. S. (1968) Masked tonal thresholds in the bottlenosed porpoise. *J. Acoust. Soc. Am*. **44**, 965–967.

Johnson, C.S. (1971) Auditory masking of one pure tone by another in the bottlenose porpoise. *J. Acoust. Soc. Am*. **49**, 1317–1318.

Johnson, C. S. (1992) Detection of tone glides by the beluga whale. In: J. A.Thomas, R. A. Kastelein & A. Ya. Supin (eds) *Marine Mammal Sensory Systems*, pp. 241–247. Plenum Press, New York.

Johnson, C. S., McManus, M. W. & Skaar D. (1989) Masked tonal hearing thresholds in the beluga whale. *J. Acoust. Soc. Am.* **85**, 2651–2654.

Nachtigall, P. E., Au, W. W. L., Pawloski, J. L. & Moore, P. W. B. (1995) Risso's dolphin (*Grampus griseus*) hearing thresholds in Kaneohe Bay, Hawaii. In: R. A. Kastelein, J. A. Thomas & P. E. Nachtigall (eds) *Sensory Systems of Aquatic Mammals*, pp. 49–54. DeSpill Publishers, Woerden, The Netherlands.

Patterson, R. D., Nimmo-Smith, I., Weber, D. L. & Milroy, R. (1982) The deterioration of hearing with age: Frequency selectivity, the critical ratio, the audiogram, and speech threshold. *J. Acoust. Soc. Am*. **72**, 1788–1803.

Popov, V. V. & Klishin, V. O. (1998) EEG study of hearing in the common dolphin, *Delphinus delphis*. *Aquatic Mammals* **24**, 13–20.

Popov, V. V., Ladygina, T. F. & Supin, A. Ya. (1986) Evoked potentials in the auditory cortex of the porpoise, *Phocoena phocoena*. *J. comp. Physiol. A* **158**, 705–711.

Popov, V. V. & Supin, A. Ya. (1987) Hearing characteristics of the white whale (in Russ.). *Dokl. Akad. Nauk SSSR* (*Proc. Acad. Sci. USSR*) **294**, 1255–1258.

Popov, V. V. & Supin, A. Ya. (1990*a*) Auditory brain stem responses in characterization of dolphin hearing. *J. Comp. Physiol. A* **166**, 385–393.

Popov, V. V. & Supin, A. Ya. (1990*b*) Electrophysiological study of hearing of the fresh-water dolphin *Inia geoffrensis* (in Russ.). *Dokl. Akad. Nauk SSSR* (*Proc. Acad. Sci. USSR*) **13**, 238–241.

Popov, V. V. & Supin, A. Ya. (1990*c*) Electrophysiological studies of hearing of some Cetaceans and a Manatee. In: J. Thomas and R. Kastelein (eds) *Sensory Abilities of Cetaceans: Laboratory and Field Evidence*. pp. 405–415. Plenum Press, New York.

Popov, V. V. & Supin, A. Ya. (1997) Detection of temporal gaps in noise in dolphins: Evoked-potential study. *J. Acoust. Soc. Am*. **102**, 1169–1176.

Popov, V. V. & Supin, A. Ya. (1998) Auditory evoked responses to rhythmic sound pulses in dolphins. *J. Comp. Physiol. A.* **183**, 519–524.

Popov, V. V., Supin, A. Ya. & Klishin, V. O. (1995) Frequency tuning curves of the dolphin's hearing: Envelope-following response study. *J. comp. Physiol. A.* **178**, 571–578.

Popov, V. V., Supin, A. Ya. & Klishin, V. O. (1997) Frequency tuning of the dolphin's hearing as revealed by auditory brain-stem response with notch-noise masking. *J. Acoust. Soc. Am*. **102**, 3795–3801.

Supin A. Ya. & Popov V. V. (1995) Envelope-following response and modulation transfer function in the dolphin's auditory system. *Hearing Res*. **92**, 38–46.

Supin, A. Ya., Popov, V. V. & Klishin, V. O. (1993) ABR frequency tuning curves in dolphins. *J. Comp. Physiol. A.* **173**, 649–656.

Szymanski, M. D., Supin, A. Ya., Bain, D. E. & Henry, K. R. (1998) Killer whale (*Orcinus orca*) auditory evoked potentials to rhythmic clicks. *Marine Mammal Sci*. **14,** 676–691.

Szymanski, M. D., Bain, D. E., Kiehl, K., Pennington, S., Wong, S. & Henry, K. R. (1999) Killer whale (*Orcinus orca*) hearing: Auditory brainstem response and behavioral audiograms. *J. Acoust. Soc. Am.* **106**, 1134–1141.

Thomas, J., Chun, N., Au, W. & Pugh, K. (1988) Underwater audiogram of a false killer whale (*Pseudorca crassidens*). *J. Acoust. Soc. Am*. **84**, 936–940.

Tremel, D. P., Thomas, J. A., Ramirez, K. T., Dye, G. S., Bachman, W. A., Orban, A. N. & Grimm, K. K. (1998) Underwater hearing sensitivity of a Pacific white-sided dolphin, *Lagenorhynchus obliquidens*. *Aquatic Mammals* **24**, 63–69.

Turl, C. W., Penner, R. H. & Au, W. W. L. (1987) Comparison of target detection capabilities of the beluga and bottlenose dolphin. *J. Acoust. Soc. Am.* **82**, 1487–1491.

Turl, C. W., Skaar, D. J. & Au, W. W. L. (1991) The echolocation ability of the beluga (*Delphinapterus leucas*) to detect target in clutter. *J. Acoust. Soc. Am.* **89**, 896–901.

Wang, D., Wang, K., Xiao, Y. & Sheng, G. (1992) Auditory sensitivity of a Chinese river dolphin, *Lipotes vexillifer*. In: J. A. Thomas, R. A. Kastelein & A. Ya. Supin (eds) *Marine Mammal Sensory Systems*, pp. 213–222. Plenum Press, New York.

White, Jr., M. J., Norris, J. C., Ljungblad, D. K., Barton, K. & di Sciara, G. N. (1978) Auditory thresholds of two beluga whales (*Delphinapterus leucas*). In: *Hubbs/Sea World Research Inst. Tech. Rep.* pp. 78–109. Hubbs Marine Research Institute, San Diego, CA.